



## Communication

## Effect of external magnetic field on the coexistence of SC and AFM in iron based superconductors

S.K. Goi<sup>a,c</sup>, B. Pradhan<sup>b,\*</sup>, Srikanta Behera<sup>b</sup>, P.K. Parida<sup>b</sup>, R.N. Mishra<sup>a</sup><sup>a</sup> Department of Physics, Ravenshaw University, Cuttack, Odisha 753003, India<sup>b</sup> Department of Physics, B.J.B. College, Bhubaneswar, Odisha 751014, India<sup>c</sup> Department of Physics, N. C. College, Jajpur, Odisha 755007, India

## ARTICLE INFO

Communicated by H. Akai

## Keywords:

A. Iron based superconductors

D. Superconductivity

D. Antiferromagnetism

D. Density of states

## ABSTRACT

We have studied the interplay of antiferromagnetism and superconductivity in presence of an applied external magnetic field for the iron based superconductors. For the purpose we have proposed a model Hamiltonian and solved it self-consistently by using the Zubarev's technique of double time Green's function technique. The self-consistent gap equations are solved numerically and interpreted the gap values from the of density of states plots.

## 1. Introduction

The interplay between superconductivity (SC) and magnetism is a long history since the discovery of superconductors. It is observed that in all the superconductors like copper oxides [1,2], heavy fermions [3,4] and iron based superconductors [5–9], the SC always appears near the antiferromagnetic (AF) order. The origin of the SC in high- $T_c$  superconductors may be understood through magnetism [10].

In this communication, we have presented a comprehensive account of AF order and its relationship with SC in iron pnictides. The magnetism play an important role in electron pairing mechanism in high- $T_c$  superconductors [10]. The senior most member of the iron pnictide superconductors  $LaFeAsO_{1-x}F_x$  was discovered, by neutron and X-ray scattering experiments, that its parent compound  $LaFeAsO$  exhibits a tetragonal to orthorhombic transition followed by a collinear AF order [11,12].

## 2. Theoretical model

The parent compounds of high- $T_c$  superconductors are AF insulators. The antiferromagnetism (AFM) plays an important role in the high- $T_c$  superconductors. On doping a suitable impurity the AF state destroys and superconducting state develops gradually in the superconductors. The AFM long range order doesn't destroys completely but continues for some higher doping in the presence of the SC. Here we proposed a model Hamiltonian to study the coexistence of AFM and SC order parameters in presence of an external magnetic field. The large

on-site Coulomb interaction between iron 3d electrons in the doped  $Fe - As$  planes suppresses almost all configurations with empty 3d orbitals and results in AFM correlation between the magnetic  $Fe$  sites. In the present model the  $Fe$  lattice has been divided into two sub-lattices A and B. The Hamiltonian to be used is of the following type.

$$H = H_0 + H_{AFM} + H_{SC} \quad (1)$$

where

$$H_0 = \sum_{k,\sigma} (\epsilon_k - sB)(a_{k,\sigma}^\dagger b_{k,\sigma} + b_{k,\sigma}^\dagger a_{k,\sigma}) \quad (2)$$

is the Hamiltonian representing the hopping of the quasi-particles between the neighbouring sites of the two sub-lattices in  $Fe - As$  planes. The electrons hopping takes place in the neighbouring  $Fe$  sites with dispersion  $\epsilon_k = -2t_0(\cos k_x + \cos k_y)$ , where  $t_0$  is the nearest neighbour hopping integral. Here  $a_{k,\sigma}^\dagger$  ( $a_{k,\sigma}$ ) and  $b_{k,\sigma}^\dagger$  ( $b_{k,\sigma}$ ) are creation (annihilation) operators of the  $Fe$  3d conduction electrons in sites A and B respectively with momentum  $k$  and spin  $\sigma$ . In the Hamiltonian,  $B$  represents the strength of applied external magnetic field and  $B = g_L \mu_B H$ , with  $g_L$  and  $\mu_B$  are the Lande  $g$ -factor for conduction electron and Bohr magnetron respectively and  $s$  is +1 for up spins and -1 for down spins. The Coulomb repulsion between  $Fe$  d-electrons is simulated by the introduction of a staggered field  $h$  which breaks the spin symmetry. The sub-lattice magnetisation arises from the Heisenberg exchange interaction between the magnetic moments at the neighbouring sites. The staggered field  $h$  acts on the  $Fe$  spins and strongly reduces the charge fluctuation. The Hamiltonian  $H_{AFM}$

\* Corresponding author.

E-mail address: [brundaban73@gmail.com](mailto:brundaban73@gmail.com) (B. Pradhan).

describes this effect.

$$H_{AFM} = h/2 \sum_{k,\sigma} s(a_{k,\sigma}^\dagger a_{k,\sigma} - b_{k,\sigma}^\dagger b_{k,\sigma}). \quad (3)$$

The AFM gap order parameter is defined as

$$h = -(1/2)g_L\mu_B \sum_{k,\sigma} s[\langle a_{k,\sigma}^\dagger a_{k,\sigma} \rangle - \langle b_{k,\sigma}^\dagger b_{k,\sigma} \rangle]. \quad (4)$$

It is believed that the superconducting gap in iron based superconductors has an s-wave symmetry which changes sign between hole and electron pockets [13–16]. But the experimental results of Zhang et al. [17] suggest that the inter-band hopping might not be so substantial. Thus, the promising candidate, the so called  $s_\pm$  wave characterized by the sign change of the superconducting orders between electron and hole pockets is not proper description of the superconducting state. Instead, the more conventional s-wave type is a more proper and general description for the iron-based superconductors. With this prescription, we assumed the inter sub-lattice superconducting pairing at two different lattice sites of *Fe* atoms, and hence the BCS type mean-field Hamiltonian is presented as

$$H_{sc} = -\Delta \sum_k (a_{k,\uparrow}^\dagger b_{-k,\downarrow}^\dagger + b_{-k,\downarrow} a_{k,\uparrow} + b_{k,\uparrow}^\dagger a_{-k,\downarrow}^\dagger + a_{-k,\downarrow} b_{k,\uparrow}). \quad (5)$$

The pairing is an s-wave type mediated by some boson mediation, other than the phonons. The inter sub-lattice pairing is not taken into consideration for simplicity of numerical calculations. The superconducting gap parameter  $\Delta$  is defined as

$$\Delta_{sc} = - \sum_k \bar{V}_k [\langle a_{k,\uparrow}^\dagger b_{-k,\downarrow}^\dagger \rangle + \langle b_{k,\uparrow}^\dagger a_{-k,\downarrow}^\dagger \rangle], \quad (6)$$

where  $\bar{V}_k$  is the effective attractive interaction in BCS limit and  $\bar{V}_k = -V_0$  for  $\epsilon_k < \hbar\omega_D$  or 0 otherwise.

### 3. Calculation of order parameters

The double time single particle electron Green's functions are calculated by using Zubarev's technique [18]. The Green's functions for the sub-lattices *A* and *B* are defined as

$$\begin{aligned} G_1(k, \omega) &= \langle\langle a_{k,\uparrow}; a_{k,\uparrow}^\dagger \rangle\rangle_\omega; G_2(k, \omega) = \langle\langle b_{-k,\downarrow}; a_{k,\uparrow}^\dagger \rangle\rangle_\omega; G_3(k, \omega) \\ &= \langle\langle b_{k,\uparrow}; b_{k,\uparrow}^\dagger \rangle\rangle_\omega; G_4(k, \omega) = \langle\langle a_{-k,\downarrow}; b_{k,\uparrow}^\dagger \rangle\rangle_\omega; G_5(k, \omega) \\ &= \langle\langle a_{k,\downarrow}; a_{k,\downarrow}^\dagger \rangle\rangle_\omega; G_6(k, \omega) = \langle\langle b_{-k,\uparrow}; a_{k,\downarrow}^\dagger \rangle\rangle_\omega; G_7(k, \omega) \\ &= \langle\langle b_{k,\downarrow}; b_{k,\downarrow}^\dagger \rangle\rangle_\omega; G_8(k, \omega) = \langle\langle a_{-k,\uparrow}; b_{k,\downarrow}^\dagger \rangle\rangle_\omega. \end{aligned} \quad (7)$$

In these Green's functions four-fold band energies  $\pm\omega_\alpha$  ( $\alpha=1$  to 4) are observed in the presence of the external magnetic field *B* as

$$\begin{aligned} \omega_1 &= -B + \sqrt{\{\epsilon_0(k) + h/2\}^2 + \Delta^2}; \omega_2 = -B - \sqrt{\{\epsilon_0(k) - h/2\}^2 + \Delta^2}, \\ \omega_3 &= -B + \sqrt{\{\epsilon_0(k) - h/2\}^2 + \Delta^2}; \omega_4 = -B - \sqrt{\{\epsilon_0(k) + h/2\}^2 + \Delta^2}. \end{aligned}$$

The AFM and SC order parameters defined in Eqns. (4) and (6) respectively are calculated from the Green's functions  $G_i$  ( $i = 1 - 8$ ). The AFM gap order parameter is

$$\begin{aligned} h &= \frac{-g_L\mu_B}{2} \sum_{k,\sigma} s[\langle a_{k,\sigma}^\dagger a_{k,\sigma} \rangle - \langle b_{k,\sigma}^\dagger b_{k,\sigma} \rangle] \\ &= \frac{-g_L\mu_B}{2} \sum_k [\langle a_{k,\uparrow}^\dagger a_{k,\uparrow} \rangle - \langle b_{k,\uparrow}^\dagger b_{k,\uparrow} \rangle - \langle a_{k,\downarrow}^\dagger a_{k,\downarrow} \rangle + \langle b_{k,\downarrow}^\dagger b_{k,\downarrow} \rangle]. \end{aligned} \quad (8)$$

Substituting the corresponding expectation values to this equation, we have

$$\begin{aligned} h &= \frac{g_L\mu_B N(0)}{2} \int_{-\frac{W}{2}}^{\frac{W}{2}} d\epsilon_k \left[ \frac{1}{\omega_1 - \omega_2} \{F_1 - F_2\} - \frac{1}{\omega_3 - \omega_4} \{F_3 - F_4\} \right] \\ \Rightarrow h &= \frac{g_1}{2} \int_{-\frac{W}{2}}^{\frac{W}{2}} d\epsilon_k \left[ \frac{1}{\omega_1 - \omega_2} \{F_1 - F_2\} - \frac{1}{\omega_3 - \omega_4} \{F_3 - F_4\} \right] \\ \Rightarrow 1 &= \frac{g_1}{2h} \int_{-\frac{W}{2}}^{\frac{W}{2}} d\epsilon_k \left[ \frac{1}{\omega_1 - \omega_2} \{F_1 - F_2\} - \frac{1}{\omega_3 - \omega_4} \{F_3 - F_4\} \right] \end{aligned} \quad (9)$$

where

$$\begin{aligned} F_1 &= (\omega_1 + B) - \{\epsilon_0(k) + h/2\} \tanh \frac{\beta\omega_1}{2}, \\ F_2 &= (\omega_2 + B) - \{\epsilon_0(k) + h/2\} \tanh \frac{\beta\omega_2}{2}, \\ F_3 &= (\omega_3 + B) - \{\epsilon_0(k) - h/2\} \tanh \frac{\beta\omega_3}{2}, \\ F_4 &= (\omega_4 + B) - \{\epsilon_0(k) - h/2\} \tanh \frac{\beta\omega_4}{2}. \end{aligned} \quad (10)$$

The SC gap order parameter is

$$\Delta_{sc} = - \sum_k \bar{V}_k [\langle a_{k,\uparrow}^\dagger b_{-k,\downarrow}^\dagger \rangle + \langle b_{k,\uparrow}^\dagger a_{-k,\downarrow}^\dagger \rangle], \quad (11)$$

where

$$\begin{aligned} \langle a_{k,\uparrow}^\dagger b_{-k,\downarrow}^\dagger \rangle &= \frac{-\Delta}{\omega_1 - \omega_2} \left[ \frac{1}{e^{\omega_1/\theta} + 1} - \frac{1}{e^{\omega_2/\theta} + 1} \right], \\ \langle b_{k,\uparrow}^\dagger a_{-k,\downarrow}^\dagger \rangle &= \frac{-\Delta}{\omega_3 - \omega_4} \left[ \frac{1}{e^{\omega_3/\theta} + 1} - \frac{1}{e^{\omega_4/\theta} + 1} \right]. \end{aligned} \quad (12)$$

$$\Rightarrow 1 = -g \int_{-\omega_D}^{\omega_D} d\epsilon_k \left[ \frac{1}{\omega_1 - \omega_2} \{F(\omega_1) - F(\omega_2)\} + \frac{1}{\omega_3 - \omega_4} \{F(\omega_3) - F(\omega_4)\} \right]. \quad (13)$$

Here, the SC coupling  $g = N(0)V_0$  and  $N(0)$  being the density of states (DOS) of conduction electrons at the Fermi surface and the integration is carried out within the cut-off energy  $\omega_D$ . In carrying out the calculation, the  $k$ -sum is replaced by an integration over energy as  $\sum_k \rightarrow N(0) \int d\epsilon_k$ . The different functions  $F(\omega_i)$  ( $i = 1$  to 4) are given by

$$\begin{aligned} F(\omega_1) &= \frac{1}{e^{\omega_1/\theta} + 1}; F(\omega_2) = \frac{1}{e^{\omega_2/\theta} + 1}, \\ F(\omega_3) &= \frac{1}{e^{\omega_3/\theta} + 1}; F(\omega_4) = \frac{1}{e^{\omega_4/\theta} + 1}. \end{aligned} \quad (14)$$

The different physical quantities of the atomic subsystem are made dimensionless by dividing the nearest neighbour hopping integral  $2t_0$ , with  $W = 8t_0$  being the width of the conduction band. The dimensionless parameters are given by

$$z = \frac{\Delta}{2t_0}, g = N(0)V_0, g_1 = N(0)g_L\mu_B, h = \frac{h}{2t_0}, x = \frac{\epsilon_k}{2t_0}, b = \frac{B}{2t_0}.$$

### 4. Results and discussion

For the numerical solutions, the coupled equations for the AFM gap parameter ( $h$ ) and the SC gap parameter ( $z$ ) are solved self-consistently. The gap functions are the functions of themselves and the other i.e., the SC gap function ( $z$ ) is a function of itself, the AFM gap function ( $h$ ) and the external magnetic field ( $b$ ) as  $z = z(z, h, b)$ . Similarly, the AFM gap function ( $h$ ) is a function of itself and others as  $h = h(z, h, b)$ . Here we have considered the half-filled band situation with the Fermi level lying at the middle of the antiferromagnetic band gap i.e., the Fermi level is taken as zero ( $\epsilon_F = 0$ ). The band width of the conduction band is considered to be  $W = 8t_0 \approx 1$  eV, where  $t_0$  is the hopping integral.

Fig. 1 shows the self-consistent plots of SC gap ( $z$ ) and AFM gap ( $h$ ) vs. reduced temperature ( $t$ ) for the SC coupling constant  $g=0.04$ , the AFM coupling constant  $g_1=0.17$  and external magnetic field  $H = 0$  T. It is observed that in the independent state, both the SC and AFM gaps

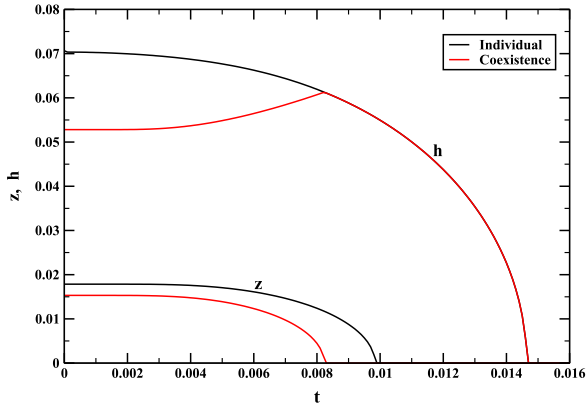


**Fig. 1.** Self-consistent plots of dimensionless SC gap ( $z$ ) and AFM gap ( $h$ ) vs. reduced temperature ( $t$ ) for the SC coupling constant  $g=0.04$ , the AFM coupling constant  $g_1=0.17$  and external magnetic field  $H = 0$  T.

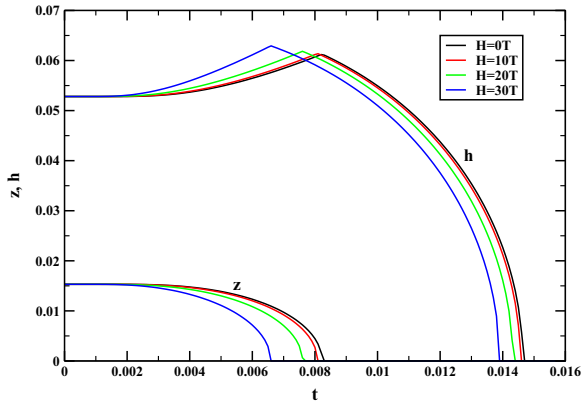


**Fig. 2.** Self-consistent plots of dimensionless SC gap ( $z$ ) and AFM gap ( $h$ ) vs. reduced temperature ( $t$ ) for fixed values of the SC coupling constant  $g=0.04$ , the AFM coupling constant  $g_1=0.17$  and different values of the external magnetic field  $H = 0$  T, 10 T, 20 T and 30 T.

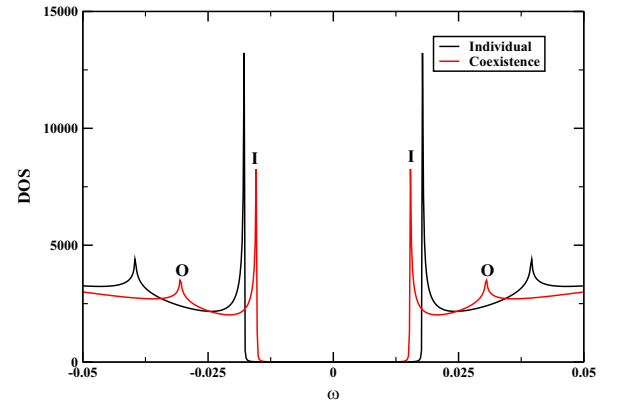


**Fig. 4.** DOS plot for independent and coexistence states at zero external magnetic field.

show mean field behaviour throughout the temperature range. The SC transition temperature  $t_c$  is 0.0099 which corresponds to  $\sim 25$  K and the Ne  $\epsilon$  l temperature  $t_N$  is 0.0147 which corresponds to  $\sim 37$  K. The reduced SC gap parameter  $2\Delta(0)/k_B T_c = 3.6$  which is comparable to the universal BCS value of 3.52. In the coexistence state, the SC gap parameter is suppressed throughout the temperature range and the reduced SC gap parameter is little enhanced to  $2\Delta(0)/k_B T_c = 3.68$ . The AFM gap parameter is suppressed within the  $t_c$  and is not changed in the pure AFM state. The AFM order state makes less number of electrons available for SC and hence the SC is suppressed.

**Fig. 2** represents the effect of the external magnetic field on the SC and AFM gap parameters. It shows that the zero temperature SC and AFM gap values does not change for any applied fields and remains almost constant at lower temperatures. The SC gap parameter is suppressed with the applied field towards higher temperatures. This effect raises the reduced SC gap parameter value  $2\Delta(0)/k_B T_c$  from 3.6 to 5.4 for the fields 0–30 T. This indicates that the SC transition temperature is reduced in presence of the applied field. Similarly the Ne  $\epsilon$  l temperature is also reduced with the applied field, however, the AFM gap parameter is slightly enhanced in the coexistence state. So the applied magnetic field destroys the SC but enhances the AFM in the coexistence state.

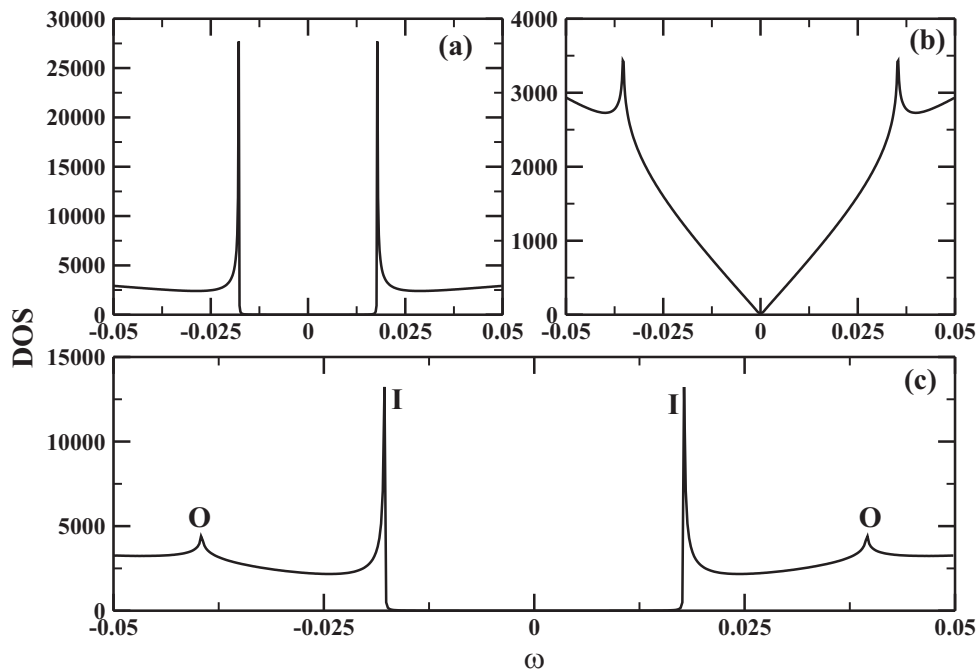


**Fig. 3.** DOS plots for (a) SC gap, (b) AFM gap and (c) combination of SC and AFM gaps in the independent state at zero external magnetic field.

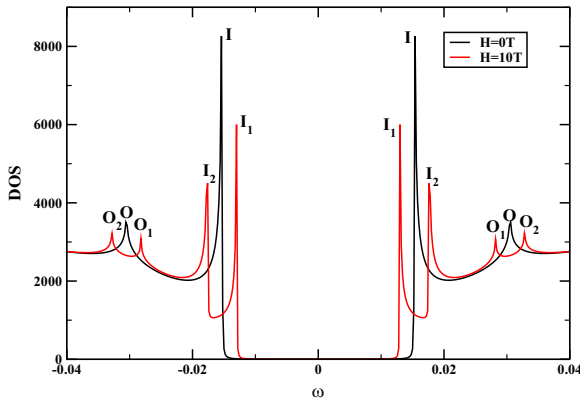


Fig. 5. DOS plots for external magnetic fields  $H = 0$  T and 10 T in the coexistence state.

The imaginary part of the single-particle electron Green's functions gives the quasi-particle DOS  $\rho(k, \omega, \sigma)$  which can be defined as  $\rho(\omega) = \sum_{k, \sigma} \rho(k, \omega, \sigma)$ . By definition  $\rho(k, \omega, \sigma) = -\frac{1}{\pi} \text{Im}\{G(k, \omega, \sigma)\}$ , where the single particle Green's function for the conduction band is  $G(k, \omega, \sigma)$  which can be found from Green's functions  $G_1(k, \omega)$  and  $G_3(k, \omega)$ . The tunneling conductance for iron based high- $T_c$  superconductors [19–22] can be calculated from the quasi-particle DOS at the Fermi surface. Fig. 3 shows the DOS plots for (a) SC gap (b) AFM gap and (c) combination of SC and AFM gaps in independent states for zero external field. The gap peaks in Fig. 3(a) appears at  $\pm 0.0178$  which resembles the SC gap  $\pm z$  value of Fig. 1. Similarly, the gap peaks in Fig. 3(b) appears at  $\pm 0.035$  which is equivalent to  $\pm h/2$  i.e., half of the AFM gap of Fig. 1. The inner peaks II of the Fig. 3(c) appears at  $\pm 0.0178$  describes the SC gap ( $z$ ) and the outer peaks OO appears at  $\pm 0.0395$  which is due to the interference of the SC and AFM gap parameters and is equivalent to  $\pm \sqrt{z^2 + (\frac{h}{2})^2}$ .

Fig. 4 shows the DOS plots for the combined individual and coexistence states of SC and AFM gaps. In both the cases the inner peaks appears at  $\pm z$  and the outer peaks appears at  $\pm \sqrt{z^2 + (\frac{h}{2})^2}$  in the absence of the applied magnetic field.

Fig. 5 shows the effect of applied magnetic field on the DOS in the coexistence state of SC and AFM. When the magnetic field is applied both the gap peaks split into two each. The outer peak OO splits into  $O_1O_1$  and  $O_2O_2$  and the inner peak II splits into  $I_1I_1$  and  $I_2I_2$ . The outer peaks  $O_1O_1$  appears at  $\pm 0.0282$  and  $O_2O_2$  at  $\pm 0.0328$  which are equivalent to  $\pm \{\sqrt{z^2 + (\frac{h}{2})^2} - b\}$  and  $\pm \{\sqrt{z^2 + (\frac{h}{2})^2} + b\}$  respectively. Similarly, the inner peaks  $I_1I_1$  appears at  $\pm 0.0130$  and  $I_2I_2$  at  $\pm 0.0176$  which are equivalent to  $\pm(z - b)$  and  $\pm(z + b)$  respectively. As a result, each gap edge is Zeeman split by the magnetic field by a separation of ( $\sim 2b$ ). Thus, the conductance curves in magnetic fields are highly asymmetrical with respect to the zero applied voltage in the tunneling experiments, indicating a strong spin polarisation in the tunnel current. This is called the spin-filter effect in a tunnel junction first observed on Au/EuS/Al junctions [23]. Where the authors have

observed the contribution of the exchange splitting in the conduction of the ferromagnetic superconductor EuS in addition to magnetic splitting.

## 5. Conclusion

In the present communication, we report the interplay of SC and AFM states in underdoped region near the on-set of SC in high- $T_c$  iron based superconductors in presence of an external magnetic field. The mean-field level calculations are carried out for SC and AFM order parameters from the model Hamiltonian by using Zubarev's technique of the single-particle double time Green's functions. The order parameters are solved self-consistently in presence of the external magnetic field. The external magnetic field decreases the reduced BCS gap value  $2\Delta_0/k_B T_c$  and the Ne  $\epsilon$  l temperature. The temperature dependence of the quasi-particle DOS represents the tunneling conductance of the scanning tunneling microscopic data. The DOS exhibits two BCS type gap structures in the coexistence phase, with the outer gap edge appearing at  $\pm \sqrt{z^2 + (\frac{h}{2})^2}$  and the inner gap edge at  $\pm z$ . The Zeeman split is observed when an external magnetic field is applied.

## References

- [1] J.G. Bednorz, K.A. Müller, Z. Phys. B 64 (1986) 189.
- [2] P.A. Lee, N. Nagaosa, X.G. Wen, Rev. Mod. Phys. 78 (2006) 17.
- [3] P. Gegenwart, Q. Si, F. Steglich, Nat. Phys. 4 (2008) 186.
- [4] G.R. Stewart, Rev. Mod. Phys. 73 (2001) 797.
- [5] Y. Kamihara, H. Hiramatsu, M. Hirano, R. Kawamura, H. Yanagi, T. Kamiya, H. Hosono, J. Am. Chem. Soc. 128 (2006) 10012.
- [6] Y. Kamihara, T. Watanabe, M. Hirano, H. Hosono, J. Am. Chem. Soc. 130 (2008) 3296.
- [7] G.R. Stewart, Rev. Mod. Phys. 83 (2011) 1589.
- [8] J.S. Wen, G.Y. Xu, G.D. Gu, J.M. Tranquada, R.J. Birgeneau, Rep. Prog. Phys. 74 (2011) 124503.
- [9] D.C. Johnston, Adv. Phys. 59 (2010) 803.
- [10] D.J. Scalapino, Rev. Mod. Phys. 84 (2012) 1383.
- [11] T. Nomura, S.W. Kim, Y. Kamihara, M. Hirano, P.V. Sushko, K. Kato, M. Takata, A.L. Shluger, H. Hosono, Supercond. Sci. Technol. 21 (2008) 125028.
- [12] C. de la Cruz, Q. Huang, J.W. Lynn, J. Li, W.R. II, J.L. Zarestky, H.A. Mook, G.F. Chen, J.L. Luo, N.L. Wang, P.C. Dai, Nature (London) 453 (2008) 899.
- [13] I.I. Mazin, D.J. Singh, M.D. Johannes, M.H. Du, Phys. Rev. Lett. 101 (2008) 057003.
- [14] K. Kuroki, S. Onari, R. Arita, H. Usui, Y. Tanaka, H. Kontani, H. Aoki, Phys. Rev. Lett. 101 (2008) 087004.
- [15] M. Khodas, A.V. Chubukov, Phys. Rev. Lett. 108 (2012) 247003.
- [16] J. Hu, Phys. Rev. X 3 (2013) 031004.
- [17] Y. Zhang, L.X. Yang, M. Xu, Z.R. Ye, F. Chen, C. He, H.C. Xu, J. Jiang, B.P. Xie, J.J. Ying, X.F. Wang, X.H. Chen, J.P. Hu, M. Matsunami, S. Kimura, D.L. Feng, Nat. Mater. 10 (2011) 273.
- [18] D.N. Zubarev, Sov. Phys. Usp. 3 (1960) 320.
- [19] Y. Zhang, L.X. Yang, M. Xu, Z.R. Ye, F. Chen, C. He, H.C. Xu, J. Jiang, B.P. Xie, J.J. Ying, X.F. Wang, X.H. Chen, J.P. Hu, M. Matsunami, S. Kimura, D.L. Feng, Nat. Mater. 10 (2011) 273.
- [20] P.M.R. Brydon, C. Timm, Phys. Rev. B 80 (2009) 174401.
- [21] T. Berlijn, C.-H. Lin, W. Garber, W. Ku, Phys. Rev. Lett. 108 (2012) 207003.
- [22] Y. Zhang, L.X. Yang, F. Chen, B. Zhou, X.F. Wang, X.H. Chen, M. Arita, K. Shimada, H. Namatame, M. Taniguchi, J.P. Hu, B.P. Xie, D.L. Feng, Phys. Rev. Lett. 105 (2010) 117003.
- [23] X. Hao, J.S. Moodera, R. Meservey, Phys. Rev. B 42 (1990) 8235.